PINNACLE ACADEMICS PRESS
*European Journal of Engineering and Technologies*

*Article*

# Lightweight Design of the Chassis and Outrigger Mechanism of an Aerial Work Platform Based on Simcenter Inspire

**Lu Zhang[1,*], Junxi Chen[1] and Xiangwei Deng[1]**

[1] University of Science and Technology Liaoning, Anshan, China
* Correspondence: Lu Zhang, University of Science and Technology Liaoning, Anshan, China

**Abstract:** To cut the excessive self-weight and redundancy of an aerial work platform's outrigger mechanism, this paper presents a lightweight workflow - multibody dynamics load extraction, finite element strength analysis, SIMP topology optimization, manufacturability-oriented reconstruction, closed-loop verification - on the integrated Siemens Simcenter Inspire platform, targeting Outrigger 1. Using extreme multibody dynamics loads as boundary conditions, topology optimization is run at a 25% design-space volume fraction under an extrusion constraint, and three reconstruction schemes are compared. After optimization the maximum von Mises stress is 195.7 MPa, the displacement 2.548 mm, and the minimum safety factor 1.1; strength meets requirements, the mass drops from 1353.921 kg to 111.911 kg (a 91.7% reduction, i.e., the remaining mass is only 8.3% of the original), and the trajectory matches the prototype without interference.

**Keywords:** aerial work platform; outrigger mechanism; lightweight design; topology optimization; Simcenter Inspire

Received: 26 May 2026
Revised: 10 July 2026
Accepted: 25 July 2026
Published: 30 July 2026



## 1. Introduction

Aerial work platforms are widely used in construction, maintenance and municipal operations; their outrigger mechanism is the key load-bearing unit for stable support and anti-overturning. Traditional outriggers mostly use solid box-welded structures with ample safety margin but excessive redundant mass, energy consumption and cost. Driven by equipment lightweighting and low-carbonization, load-path-based topology optimization has become an effective way to remove redundancy and improve performance [1-2]. Integrated platforms such as Siemens Simcenter Inspire combine multibody dynamics, finite element analysis and topology optimization, lowering the barrier to lightweight design [3-4]. The approach has been applied to construction-machinery components, such as excavator booms and working devices and to hydraulic manipulators [5]. Using Simcenter Inspire, this paper conducts the lightweight design of the outrigger mechanism with whole-vehicle (chassis-level) verification.

## 2. Model Establishment and Multibody Motion Simulation

### *2.1. Material Definition and Properties*

Following the construction-machinery convention, the cylinder rod (CT2026-1) and sleeve (CT2026-2) use quenched-and-tempered alloy structural steel, the ground (CT2026-3) uses C50 concrete, and the main load-bearing members (e.g., the outrigger body) adopt European-standard S355JR low-alloy high-strength steel (Chinese Q355). Their mechanical properties are listed in Table 1.

**Table 1.** Material Property Parameters of Each Part of the Outrigger Mechanism

| Part | Grade | Corresponding real material | E / MPa | ν | ϱ / (kg·mm⁻³) | σ_s / MPa |
|---|---|---|---|---|---|---|
| Cylinder rod | CT2026-1 | quenched-and-tempered alloy steel (40Cr/42CrMo grade) | $2.0\times10^{5}$ | 0.30 | $7.1\times10^{-6}$ | 380 |
| Cylinder sleeve | CT2026-2 | High-grade alloy steel (42CrMo grade) | $2.0\times10^{5}$ | 0.30 | $7.1\times10^{-6}$ | 420 |
| Ground | CT2026-3 | C50 concrete | $3.0\times10^{4}$ | 0.20 | $2.4\times10^{-6}$ | 50 |
| Other structural members | S355JR | European-standard structural steel (Chinese standard Q355) | $2.1\times10^{5}$ | 0.29 | $7.85\times10^{-6}$ | 355 |

Note 1: CT2026-1/2/3 are designated grades for the studied object, corresponding respectively to the quenched-and-tempered alloy steel for construction-machinery cylinders, the high-grade alloy steel for cylinder sleeves, and C50 concrete; their mechanical parameters serve as the material input for the finite element simulation.
Note 2: The density of CT2026-1/2 is taken as 7.1×10−6 kg/mm3 (7100 kg/m3), slightly lower than that of ordinary carbon steel (about 7850 kg/m3); this is a designated material parameter and is adopted as such in this paper.

*2.2. Model Import and Connection Setup*

The whole-machine model is imported in the MMKS (mm·kg·N·s) system; 4 rigid-body groups are built (4 cylindrical, 4 planar and 32 pin joints), and 4 step-dwell-step translational drivers are set (250 mm, 0--5 s, 30 Hz). An external 2000 N load is applied along -Y at frame point A (-963, 500, 0), gravity along -Y. A 0--5 s multibody dynamics simulation yields the Outrigger 1 midpoint trajectory and 5 extreme-load conditions as the load input.

## 3. Initial Strength Analysis and Redundancy Identification

Under the linear-elastic small-deformation assumption and the fourth strength theory (von Mises criterion), with OptiStruct as the solver and a 20 mm element size, an initial strength analysis of Outrigger 1 is performed using the 5 maximum connection loads; results are given by the von Mises equivalent stress. The maximum von Mises stress is 192.6 MPa and the maximum displacement 0.6014 mm (Figure 1). The original outrigger has ample strength reserve but an extremely unbalanced stress distribution - most of the box section lies in the low-stress region - indicating large lightweighting potential.

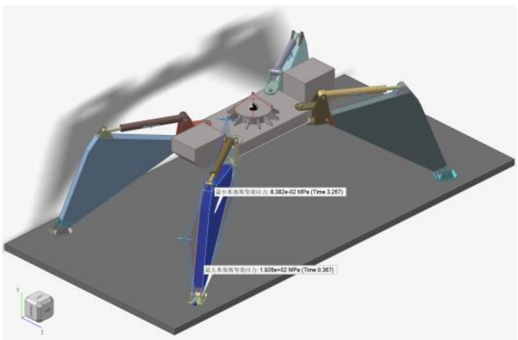

**Figure 1.** Initial Strength Analysis (Maximum Stress 192.6 MPa)

Preliminary Selection of Configuration Schemes: Before setting the mass target, two schemes are compared: Scheme 1 is a triangular closed-section with inner stiffener plates (occupying 25% of the design space, high lightweighting potential, good formability for extrusion); Scheme 2 is an open section without stiffener plates (35% occupancy, low potential, only fair formability).

Scheme 2 is thus inferior to Scheme 1 in both volume occupancy and mass-reduction potential, with poorer formability; therefore, the subsequent topology optimization is carried out on the basis of Scheme 1 with a 25% volume fraction (the topology-optimization volume constraint) as the constraint.

## 4. Topology Optimization

Based on the SIMP (Solid Isotropic Material with Penalization) variable-density method, with the element relative density $\rho_e$ as the design variable and minimum compliance as the objective. The material interpolation model uses a penalty factor p to drive the density toward two extremes

$$E_e(\rho_e) = E_{min} + \rho_e^p(E_0 - E_{min})$$

The optimization problem is formulated as: minimize the compliance under a volume constraint,

$$\min c(\rho) = \sum_e \rho_e^p u_e^T k_e u_e\,, \qquad \frac{V(\rho)}{V_0} \leq f$$

Where $V_0$ is the initial design-space volume and f the upper volume-fraction limit (taken as 25%). The outrigger body is the design space; the pre-partitioned non-design space is fixed, and an extrusion constraint (thickness 53--107.985 mm) avoids undercuts and enclosed cavities. Loads are the 5 extreme conditions from multibody dynamics. The result retains each hinge-seat region and replaces the solid with bionic bridge-like ribs, forming a 'multi-path load transfer + voided mass reduction' configuration (Figure 2).

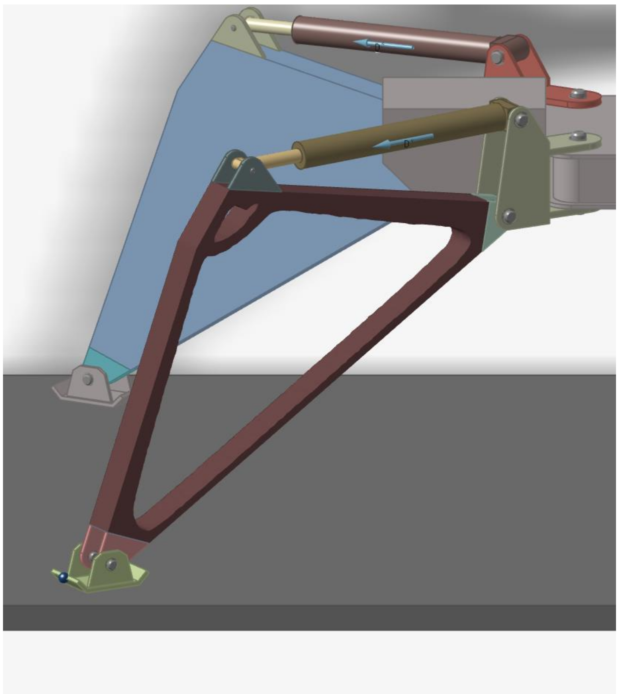

**Figure 2.** Topology Optimization Conceptual Model of Outrigger 1 (Volume Fraction 25%)

## 5. Geometric Reconstruction and Scheme Comparison

Following Design for Manufacturability (DFM), the cross-section is extracted along the extrusion direction, the main load-transfer region is reinforced, low-stress regions are simplified with fillet transitions, and a manual fitting reconstruction is performed. The extrusion constraint also enforces a wall-thickness range of 53-107.985 mm, satisfying the minimum-wall-thickness requirement of Design for Manufacturability. Based on the 25% topology model, three configurations are compared: Scheme 11 with voided support, Scheme 12 without stiffener plates, Scheme 13 with stiffener-plate support.

As the comparison shows: Scheme 11 (voided support) reaches a maximum von Mises stress of 195.7 MPa at 111.911 kg with good torsional performance; Scheme 12 has the lowest stress (189.7 MPa) but a much larger mass (276.532 kg) and poor torsion; Scheme 13 (stiffener-plate support) is the heaviest (290.762 kg) and most stressed (257.3 MPa), with obvious redundancy. Balancing mass reduction and feasibility, Scheme 11 is selected as the final model (Figure 3).

**Figure 3.** Final Reconstructed Model of Scheme 11 (Voided Support)

**6. Verification**

The reconstructed outrigger is substituted into the original-machine model (single-variable principle) with the initial parameters; a motion-simulation verification shows the Outrigger 1 trajectory coincides fully with no interference. After Boolean-merge replacement of Outriggers 2/3/4, a whole-vehicle strength verification gives a maximum stress of 195.7 MPa, displacement 2.548 mm and minimum safety factor 1.1, meeting the design requirements and confirming the lightweight design (As shown in Table 2).

**Table 2.** Performance Comparison Before and After Optimization (91.7% Mass Reduction) Note: The Minimum Safety Factor (1.1) Is the Local Value at the Outrigger End-Hinge (a Stress-Concentration Region), Whereas the Maximum Von Mises Stress (195.7 MPa) Is the Global Maximum; the Two Are Taken at Different Locations.

| Metric | Initial | Optimized |
|---|---|---|
| Maximum von Mises stress / MPa | 192.6 | 195.7 |
| Maximum displacement / mm | 0.6014 | 2.548 |
| Minimum safety factor | 1.8 | 1.1 |
| Outrigger mass / kg | 1353.921 | 111.911 |

Figure 4 shows the whole-machine von Mises stress contour of Scheme 11 in Simcenter Inspire at t=4.667 s, peaking at $1.957\times10^2$ MPa near the Outrigger 1 end hinge, consistent with the single-outrigger independent-simulation analysis. The whole-machine safety factor ranges from a minimum of 1.1 to a maximum of 783.8; against the 355 MPa yield limit of the S355JR main member (nominal $n\approx1.81$), the local factor at the outrigger end is lower and near-critical, suggesting further study by post-processing or local rib reinforcement. The maximum displacement is 2.548 mm at the Outrigger 1 end, matching the single-outrigger independent-simulation analysis. The small difference from the single-outrigger maximum stress of 192.6 MPa arises from the different boundary conditions (isolated outrigger versus installed in the full machine) and is expected.

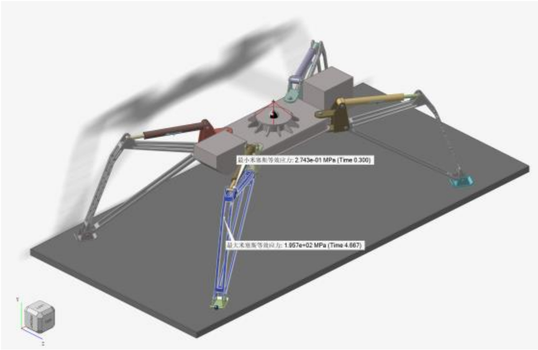

**Figure 4.** Whole-machine Von Mises Equivalent Stress Contour (Maximum 1.957×102 MPa, T=4.667 S)

### 7. Conclusion

On a single Simcenter Inspire platform this paper completes the full workflow - load extraction, strength analysis, topology optimization, engineering reconstruction, closed-loop verification - avoiding multi-software data deviation. Guided by the actual load path, it removes redundancy precisely and cuts the outrigger mass by 91.7% (the remaining mass is only 8.3% of the original) while meeting strength requirements, balancing manufacturability with torsional performance. Future work may add modal, fatigue and multi-objective studies and extend the method to crane-like telescopic members.

### References


1. O. Sigmund, “A 99 line topology optimization code written in Matlab,” *Structural and Multidisciplinary Optimization*, vol. 21, pp. 120–127, 2001, doi: 10.1007/s001580050176.
2. D. Kim, B. S. Lazarov, T. M. Surowiec, B. Keith, “A Simple Introduction to the SiMPL Method for Density-Based Topology Optimization,” arXiv preprint arXiv:2411.19421, 2025.
3. H. Wu, X. Ding, G. Liu, X. Zhu, and H. Wang, “Structural optimization of the excavator boom under extreme working conditions using EDEM-ADAMS coupled simulation,” *PLoS ONE*, vol. 20, no. 11, p. e0337421, 2025, doi: 10.1371/journal.pone.0337421.
4. H. Zhang, X. Shao, M. Jia, X. Ge, and Y. Li, “Topology optimization design of excavator working device based on equivalent static loads,” *Scientific Reports*, vol. 16, p. 13054, 2026, doi: 10.1038/s41598-026-43544-2.
5. W. Pang, Y. Chai, H. Liu, and F. Li, “Nonlinear vibration characteristics of a hydraulic manipulator model: theory and experiment,” *Journal of Vibration Engineering & Technologies*, vol. 11, pp. 1765–1775, 2023, doi: 10.1007/s42417-022-00669-8.
6. A. Cascino, L. Giannelli, E. Meli, and A. Rindi, “Integration of fatigue life assessment into structural optimization of a railway vehicle bogie frame: development and application of a new methodology,” *Railway Engineering Science*, 2026, doi: 10.1007/s40534-026-00433-8.
7. G. Zhang, X. Cui, Y. Zang, Y. Zhou, J. Lu, Z. Li, H. Yang, J. Wang, Z. Ye, R. Li, and L. Zhou, “Topology optimization of wheel spoke cavities for lightweight design under bending fatigue and impact load cases,” *Scientific Reports*, vol. 16, p. 10817, 2026, doi: 10.1038/s41598-026-46183-9.